

Support information

Ultrathin MnO₂ Nanosheets Grown on Fungal Conidium-derived Hollow Carbon Spheres as Supercapacitor Electrodes

Cuiping Mao,^{ab} Sangui Liu,^{ab} Lei Pang,^{ab} Qi Sun,^c Yang Liu,^c Maowen Xu,^{*ab} and Zhisong Lu^{*ab}

^a Chongqing Key Laboratory for Advanced Materials & Technologies of Clean Energies, Southwest University, 1 Tiansheng Road, Chongqing 400715, P. R. China

^b Institute for Clean Energy & Advanced Materials, Faculty of Materials & Energy, Southwest University, 1 Tiansheng Road, Chongqing 400715, P. R. China

^c Institute of Agro-Products Processing Science and Technology, Chinese Academy of Agricultural Sciences/Key Laboratory of Agro-Products Processing, Ministry of Agriculture, No. 2 Yuan Ming Yuan West Road, Beijing 100193, P. R. China

*: Author to whom correspondence should be addressed. Tel.: +86-23-68254732; Fax: +86-23-68254969. E-mail: zslu@swu.edu.cn or xumaowen@swu.edu.cn.

Support information

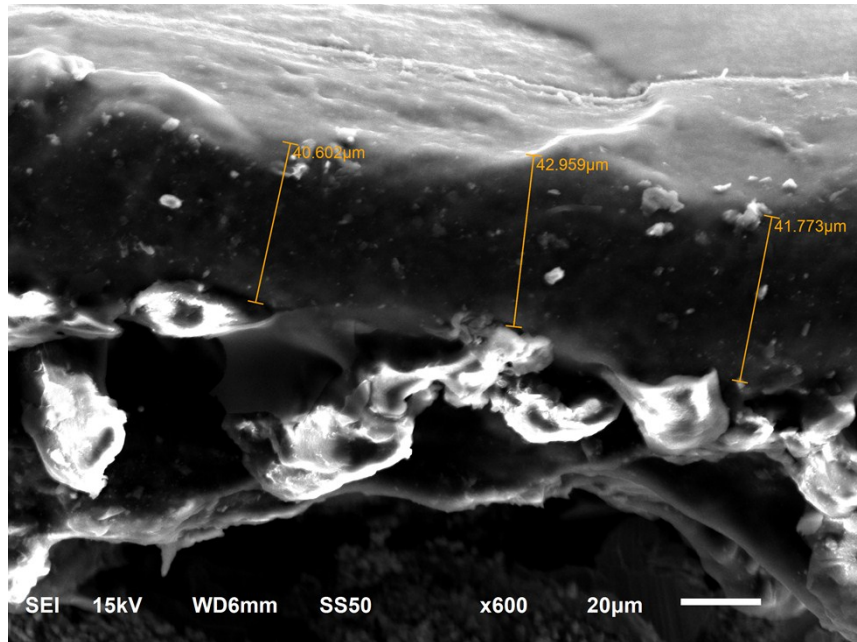


Figure S1. Cross-section SEM image of MnO₂@CC composites on the nickel form.

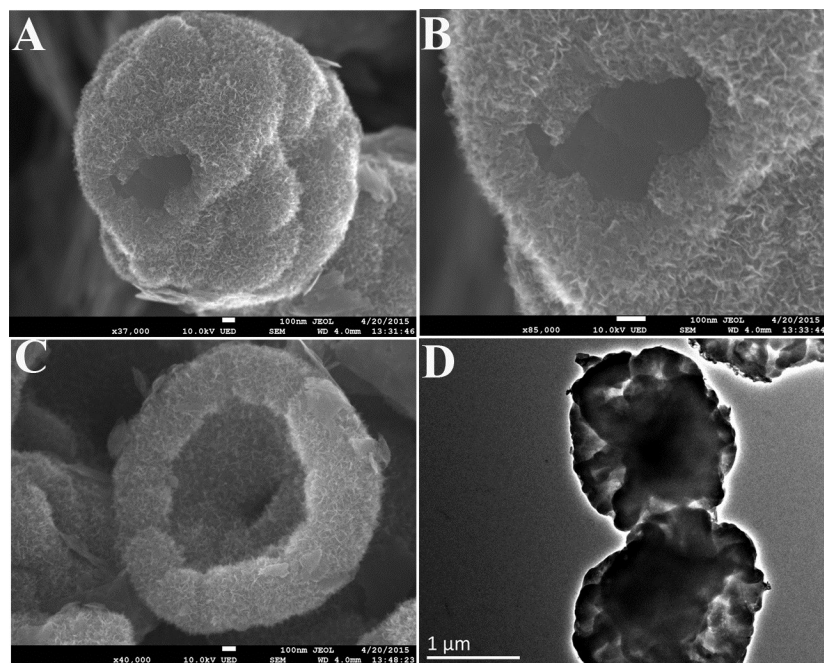


Figure S2. FESEM and TEM image of conidium-derived hollow carbon spheres.

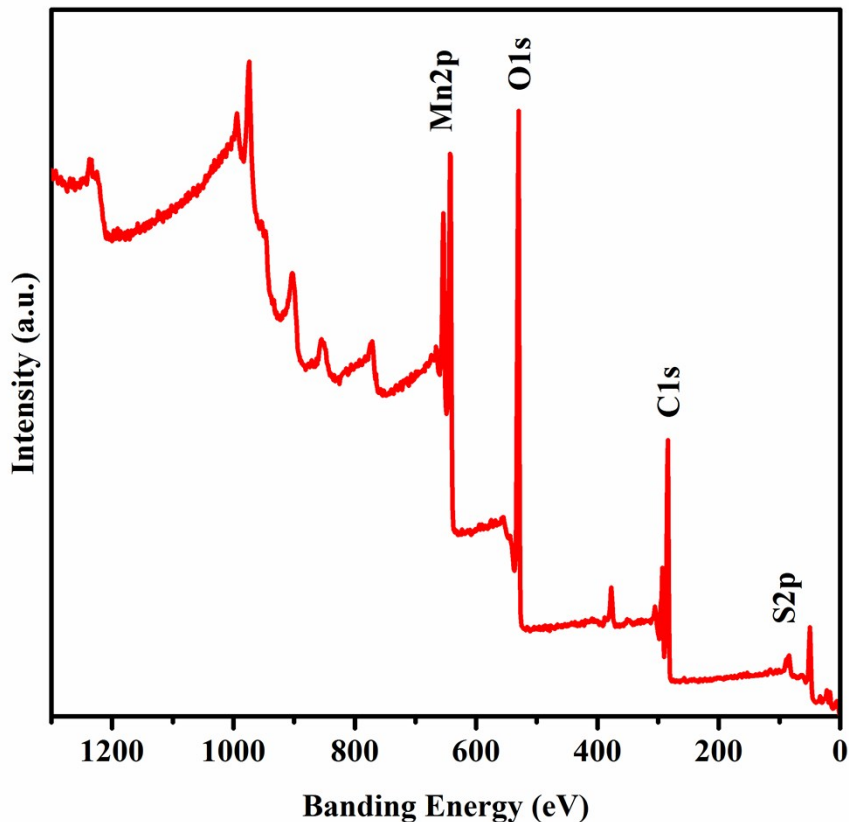


Figure S3. Survey spectrum of $\text{MnO}_2@\text{CC}$.

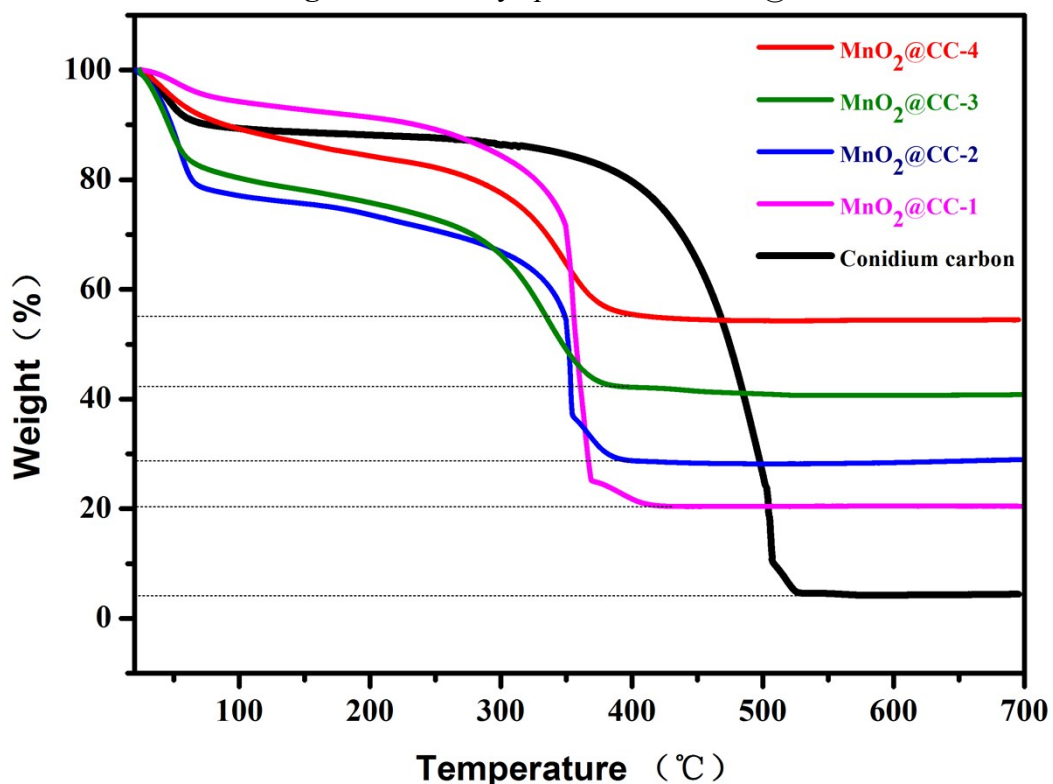


Figure S4. TGA curves of conidium carbon and $\text{MnO}_2@\text{CC}$ composites.

Support information

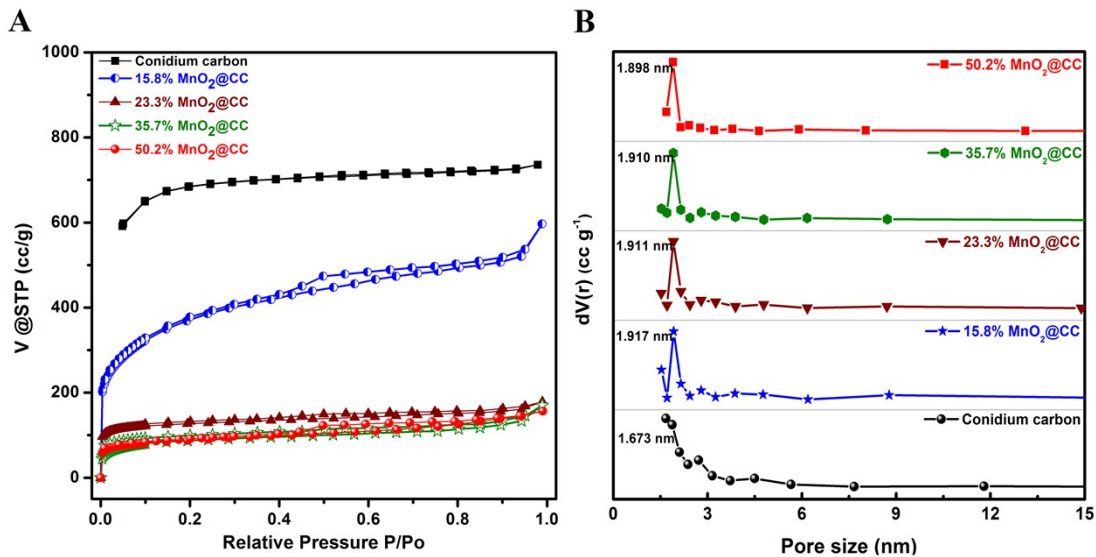


Figure S5. N₂ adsorption–desorption isotherms (A) and the corresponding pore size distribution (B) of conidium-derived and MnO₂@CC composites

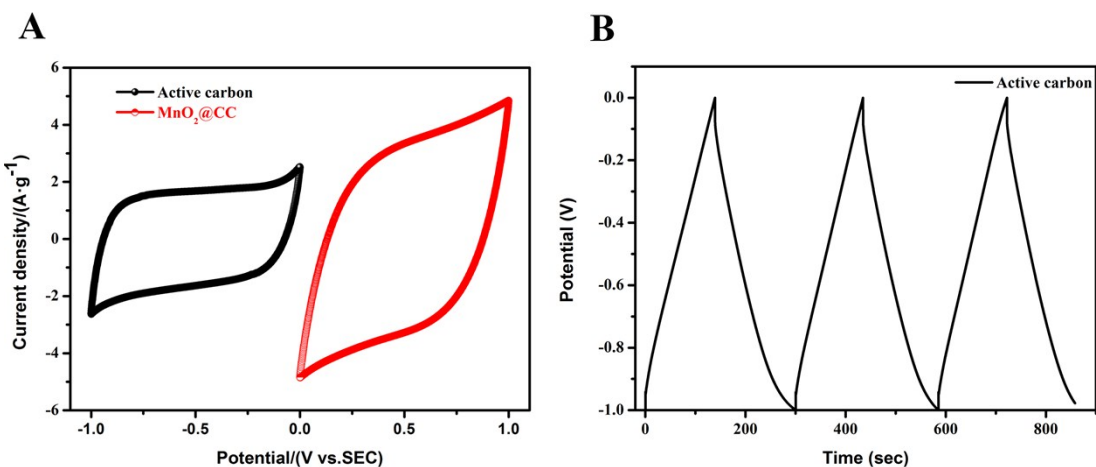


Figure S6. CV curves of active carbon and MnO₂@CC composites recorded in a three-electrode cell.

Support information

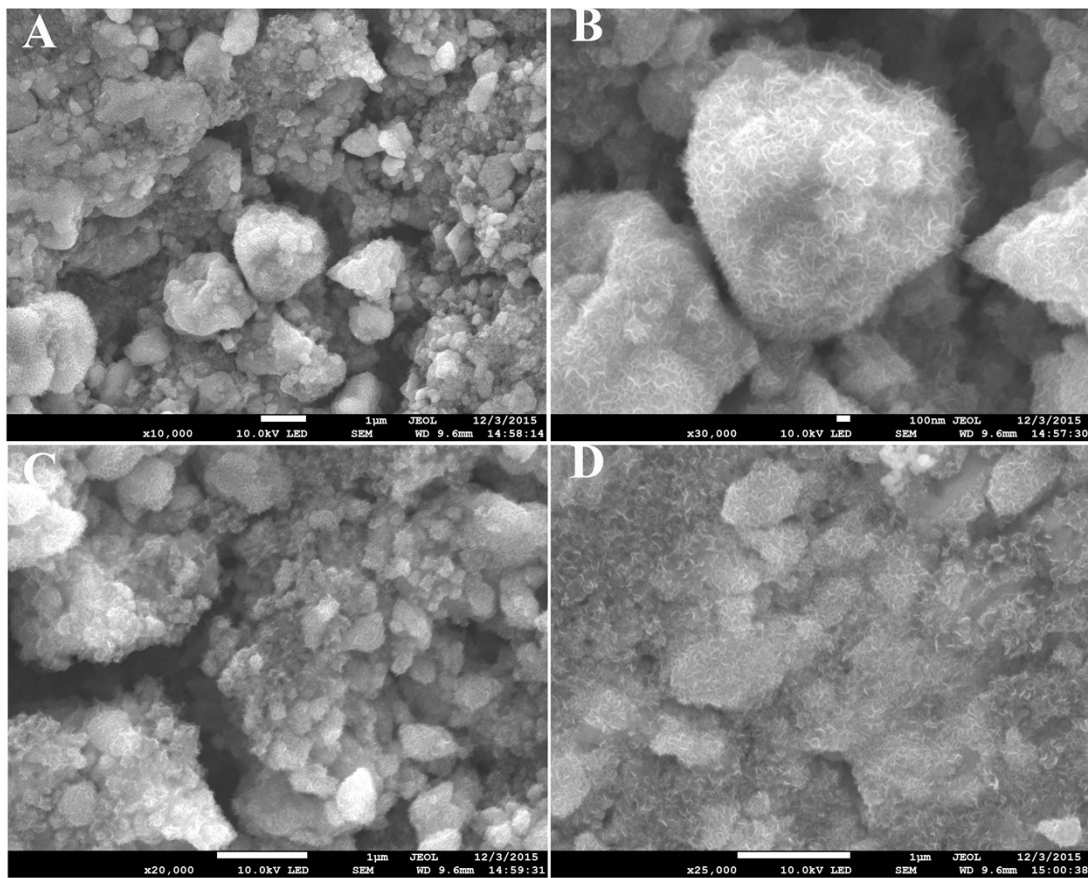
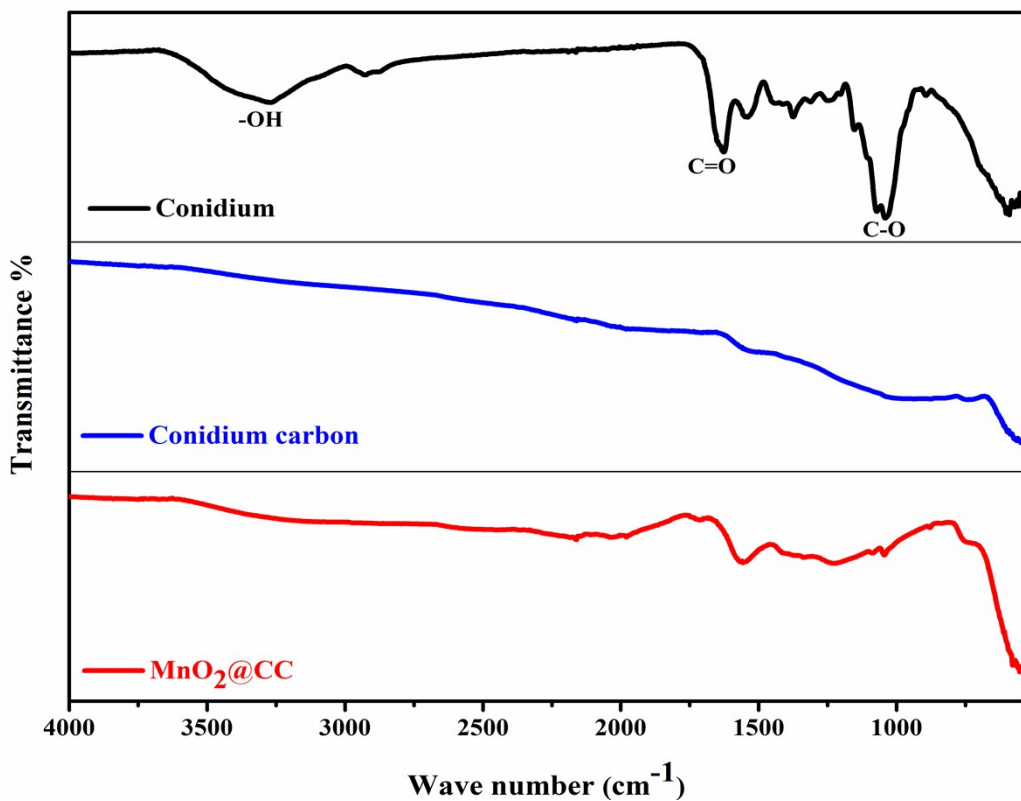


Figure S7. FESEM images of $\text{MnO}_2@\text{CC}$ composites after 1000 cycles in asymmetric supercapacitor.



Support information

Figure S8. FTIR spectra of the samples.

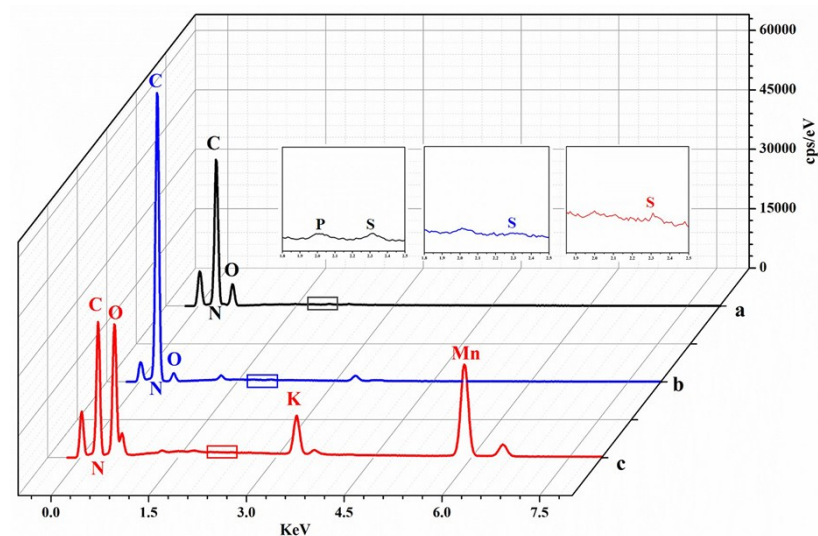


Figure S9. EDS spectra of $\text{MnO}_2@\text{CC}$.

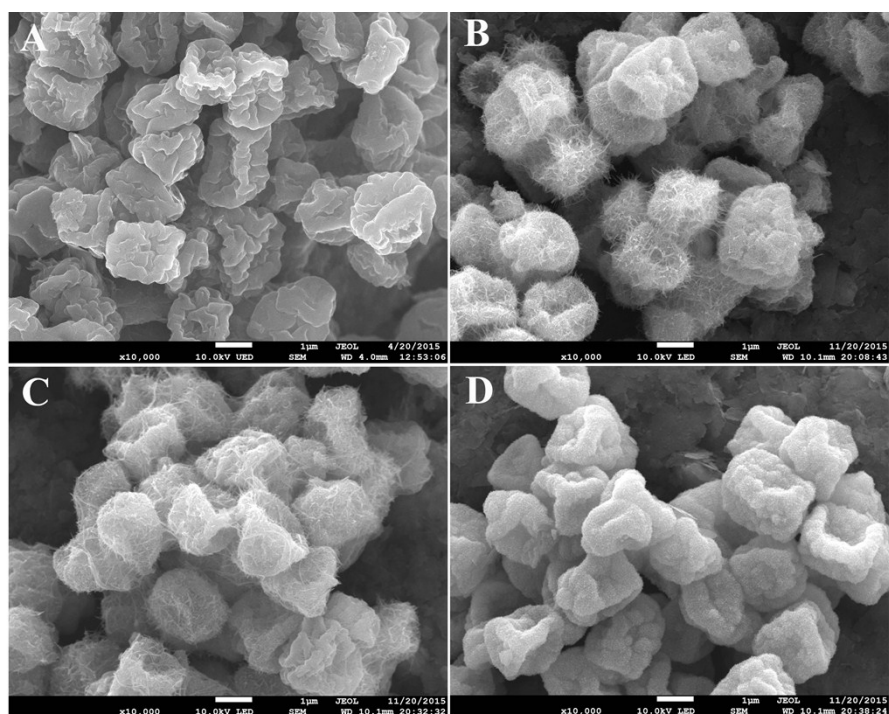


Figure S10. FESEM images of conidium carbon and $\text{MnO}_2@\text{CC}$ composites: (A) conidium carbon, (B) 15.8% $\text{MnO}_2@\text{CC}$ composites, (C) 23.3% $\text{MnO}_2@\text{CC}$ composites, (D) 35.7% $\text{MnO}_2@\text{CC}$ composites

Support information

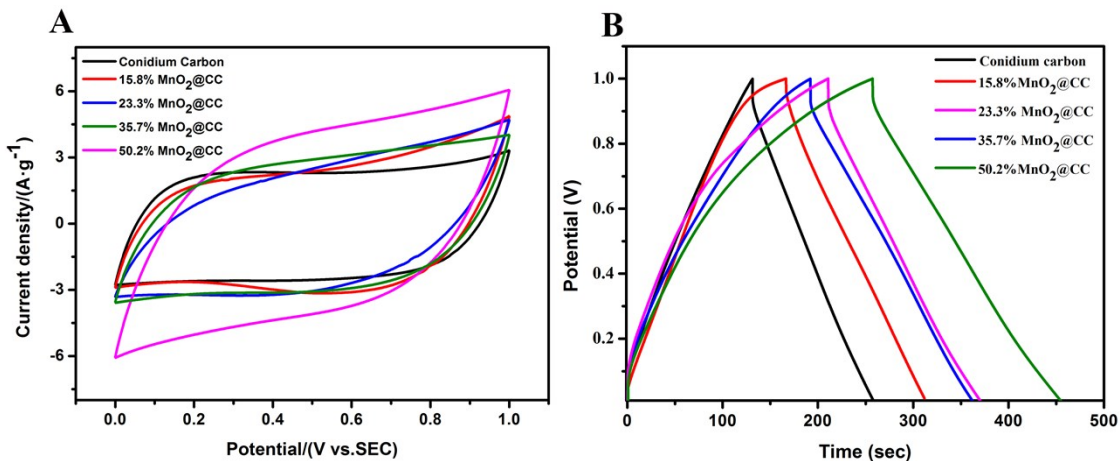


Figure S11. (A) CV curves of conidium carbon and MnO_2 @CC composites at the scan speed of 20 mV/s; (B) Galvanostatic charge/discharge curves at a current density of 1 A/g for conidium carbon and MnO_2 @CC composites.

Table 1 Characterization of different content of MnO_2 in the composites

Samples	Content of MnO_2 (wt%)	S_{BET} ($\text{m}^2 \text{g}^{-1}$)	Pore size (nm)	Specific capacitance (F g^{-1})
Conidium carbon	0	2123.96	1.67	107.8
MnO_2 @CC-1	15.8	1362.98	1.91	147.4
MnO_2 @CC-2	23.3	484.53	1.91	160.0
MnO_2 @CC-3	35.7	337.90	1.91	172.5
MnO_2 @CC-4	50.2	324.08	1.90	263.5

Support information

Table S2 Comparison of the specific capacitances of MnO₂ and MnO₂-carbon composites electrodes

Materials	Specific capacitance (F g ⁻¹)	Electrolyte	Ref.
Crystalline MnO ₂	110 (2mV/s)	0.1 M K ₂ SO ₄	1
MnO ₂ Nanorods	201 (10 mV/s)	0.5 M Li ₂ SO ₄	2
3D Manganese Oxide Nanoflowers	121.5 (5mV/s)	6 M KOH	3
Needle-like MnO ₂	233.5(100mV/s)	1 M Na ₂ SO ₄	4
Manganese Oxide Nanorod	140(1mV/s)	1 M Na ₂ SO ₄	5
Manganese oxide films	230.5(25 mV/s)	1 M Na ₂ SO ₄	6
MnO ₂ loaded biomass carbonaceous aerogel composites (MnO ₂ @CA)	123.5 (5 mV/s)	6 M KOH	7
MnO ₂ dipped biomass carbon skeleton from Lotus Pollen (MnO ₂ /C)	257 (0.5 A/g)	1 M Na ₂ SO ₄	8
MnO ₂ loaded Bacterial-Cellulose-Derived Carbon (p-BC@MnO ₂ // p-BC@MnO ₂)	256.7(1.0 A/g)	1 M Na ₂ SO ₄	9
MnO ₂ -doped, polyaniline-grafted rice husk ash nanocomposites (PANI/MnO ₂ /RHA)	135 (0.5 mA/g)	0.5 M Na ₂ SO ₄	10
MnO ₂ grown on Fungal Conidium-derived Hollow Carbon Spheres(MnO ₂ @CC)	263.5 (1.0 A/g)	1 M Na ₂ SO ₄	Our work

Support information

Reference

1. T. Brousse, M. Toupin, R. Dugas, L. Athouël, O. Crosnier and D. Bélanger, *J. Electrochem. Soc.*, 2006, **153**, A2171.
2. Q. Qu, P. Zhang , B. Wang, Y. Chen, S. Tian, Y. Wu and R. Holze, *J. Phys. Chem. C*, 2009, **113**, 14020-14027.
3. J. Ni, W. Lu, L. Zhang, Y. Yue, X. Shang and Y. Lv, *J. Phys. Chem. C*, 2008, **113**, 54-60.
4. S. Chen, J. Zhu, Q. Han, Z. Zheng, Y. Yang and X. Wang, *Cryst. Growth Des.*, 2009, **9**, 4356-4361.
5. k. Kuratani, k. Tatsumi, and N. Kuriyama, *Cryst. Growth Des.*, 2007, **7**, 1375-1377.
6. C. -K. Lin, K. -H. Chuang, C. -Y. Lin, C. -Y. Tsay, C. -Y. Chen, *Surf. Coat. Tech.*, 2007, **202**, 1272-1276.
7. Y. Ren, Q. Xu, J. Zhang, H. Yang, B. Wang, D. Yang, J. Hu and Z. Liu, *ACS Appl. Mater. Interfaces*, 2014, **6**, 9689-9697.
8. H. Li, B. Wang, X. He, J. Xiao, H. Zhang, Q. Liu, J. Liu, J. Wang, L. Liu, P. Wang, *J. Mater. Chem. A*, 2015, **3**, 9754-9762.
9. L. F. Chen, Z. H. Huang, H. W. Liang, Q. F. Guan and S. H. Yu, *Adv. Mater.*, 2013, **25**, 4746-4752.
10. P. Prabunathan, K. Sethuraman and M. Alagar, *RSC Adv.*, 2014, **4**, 47726